A Sliding Mode Control of a Hybrid Magnetic Bearing for Wayside Flywheel Energy Storage Systems

Mohamed S. Kandil, Maxime R. Dubois, João P. Trovão
e-TESC Laboratory
Departement of Electrical & Computer Engineering
Université de Sherbrooke,Sherbrooke (Qc), Canada
{M.Kandil; Maxime.Dubois; Joao.Trovao}@USherbrooke.ca

Loicq S. Bakay
Alstom Power
Sorel-Tracy (Qc), Canada
loicqbakay@gmail.com

***Abstract*—Recently, rail transportation agencies have been giving great interest to installing wayside energy storage systems (WESS) to store (for a short period of time) and recycle back the energy generated from regenerative braking systems. For economical and technical purposes, it is important to look for facilities to store energy for longer terms. Although a flywheel energy storage system is a promising technology for short period applications, the self-discharge problem impedes them from being applied in keeping energy for long periods. Magnetic bearings could be a good solution to improve the storability of FESS. However, they themselves could be a source for power loss. Thus hybrid magnetic bearings (HMB) are optimal solution for long-term FESS. To compensate the non-linear behavior of HMB, a sliding mode controller is proposed for stabilizing a rotor-HMB systems. Simulation results and a comparison to the decentralized PID controller with respect to the attenuation of rotor unbalance vibrations are presented.**

Keywords-Long-Term Wayside Flywheel Energy Storage, Magnetic Bearings, Sliding Mode Control

I. INTRODUCTION

In rail transit systems, energy storage can be sited both onboard transit vehicles, and in stationary modules on the rail wayside, termed wayside energy storage systems (WESS) [1]. In the recent years, we have witnessed a considerable interest in the utilization of WESS for electrified rail systems as an innovative solution to confront the high increase in electricity costs as well as the rise in the total number of rail rides [1], [2]. These efforts have focused on the application of WESS for two main applications; voltage regulation and absorption of the locomotives braking energy. Furthermore, WESS can be enhanced to maintain its energy for longer terms and be used for other applications such as peak shaving or help the integration of renewable energies. Additionally, WESS could be used for peak load shaving by charging with the off-peak rates at night and by discharging during the peak hours when the prices are high. This way, the transit agencies could reduce their electricity bill and avoid installing additional substation to supply the peaks of highly variable loads.

The existing projects of WESS for rail systems use three main technologies: chemical batteries, ultracapacitors and flywheels[1]. Superconducting magnetic energy storage technology is another possibility, but still undergoing advanced development [3]. Selecting the most appropriate type of energy storage for a certain application is not trivial. Based on recent studies [3]–[7], flywheel energy storage system (FESS) represents an interesting option with respect to energy efficiency, power density and life-cycle. Another possible application of FESS, also related to electric transportation, is to provide the short-term peak power demanded by level 3 fast chargers for Electric Vehicles (EV) [8].

In all cases, the self-discharge problem (rotational speed reduction at no-load) is the main obstacle for implementing Flywheels in storing energy for long periods. Losses associated to the mechanical bearings are the main contributors in the high self-discharge rate of Flywheels and subsequently impede FESS to be employed for long-term energy storage applications. In order to achieve high energy-efficient FESS storing energy for hours (e.g. 12 hours at 80% load efficiency [9]), it is necessary to reduce these losses as much as possible. Magnetic bearings and vacuum containment can be used to reduce to minimum the friction losses that cause the rotor to slow down. On the other hand, these techniques can be a source of other types of losses when including the power provided to the active magnetic bearings or when cooling superconducting bearings. Therefore, a compromise shall be made to ensure that there is a net reduction in standby losses. Bakay *et al.*[10] studied a promising homopolar HMB proposed by Sortore *et al.* in [11], see Fig. 1. This design has the ability of substantially decreasing the bearing losses.

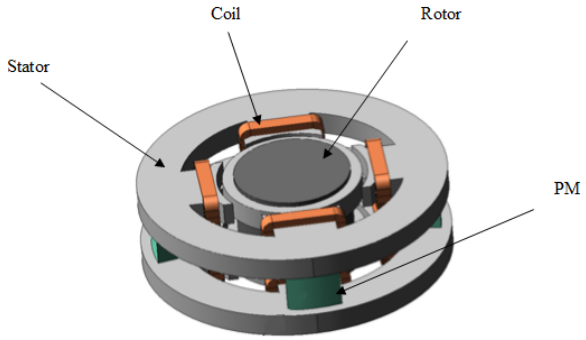

Fig. 1. Permanent magnet biased radial HMB

978-1-4673-7637-2/15/$31.00 ©2015 IEEE

In the HMB, permanent magnets (PM) are used to provide the bias flux and hence lead to lower copper losses unlike the commonly used pure Active Magnetic Bearings (AMB) which employ a fixed DC bias current. While the electromagnetic coils of the HMB are provided for regulation. In the homopolar configuration of Fig. 1, the flux density keeps the same polarity in the axial direction (parallel to the axis of rotation). Subsequently, this design has less iron losses besides having smaller coils and less copper losses than the heteropolar counterpart. Simulations showed that this solution consumes significantly less power than pure AMB [10] and leads to lower self-discharge. Moreover, homopolar HMB will lead to higher reliability and extended lifetime of the power amplifier since the required amount of power is reduced. However, this approach is somewhat more complex to build on one hand. On the other hand, the homopolar HMB is a nonlinear, unstable, multivariable system, which requires advanced controlling methods. The modeling and control of this magnetic bearing are the focus of this paper.

In past literature, decentralized PID control schemes could be used for regulating rigid rotors suspended with Active Magnetic Bearing (AMB) systems, with the advantage of simplicity in tuning their parameters [11]–[13]. Even though AMBs have no PM and are more easily controllable and more common than HMB, the performance of these simple PID controllers could degrade with higher rotational speeds because of vibration forces. Thus different unbalance and vibration compensation schemes have been developed to be implemented in conjunction with PID controllers [13]. Despite the fact that these unbalance compensation methods are powerful in reducing the vibration levels of rotor-magnetic bearing systems, they can affect the stability of the system when not appropriately designed. The last draft of the American Petroleum Institute (API) standard for machinery with AMBs does not recommend using vibration compensation methods for new installations [14]. Therefore the transition from simple PID controllers to higher performance and more robust methods seems inevitable. In the case of PM-biased HMB, the behavior is even more complex, which requires even more advanced control methods. In this paper, a decentralized single input single output sliding mode controller (SMC) for a rigid rotor supported horizontally with a radial HMB is addressed. Modeling of the rotor-HMB system is presented first. The design method of the SMC is then presented. Simulation results of the SMC and the decentralized PID controller are given, followed by the performance evaluation regarding output tracking and vibration attenuation for both controllers.

II. MATHEMATICAL MODEL

Fig.2 shows a picture of the HMB test rig used in this research project for achieving low losses in Wayside Energy Storage. One terminal of the shaft is supported by a radial PM-biased HMB while the other terminal is supported by a mechanical ball bearing. In a complete system, the axis will be suspended using two HMBs, but in the course of this paper, only one HMB is considered for simplification. The rotation is realized through an induction motor which is connected to one end of the shaft by the means of a flexible coupling.

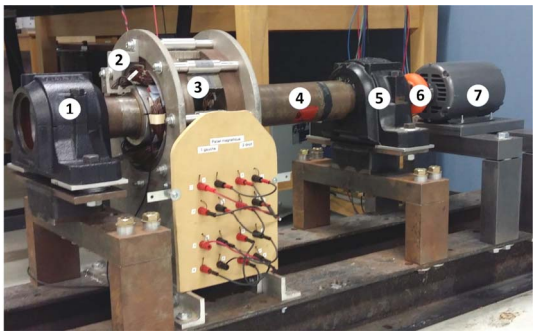

Fig. 2.Radial HMB test rig: (1) Safety bearing, (2) Position sensor, (3) HMB, (4) Shaft, (5) Ball bearing, (6) Flexible coupling, (7) Induction Motor.

The shaft displacements in both the horizontal and vertical directions are measured by two inductive position sensors. In this section, a complete mathematical model of the bearing supporting forces is presented.

A. Electromagnetic Forces

The radial HMB have two lamination stacks of four teeth each. In between the two lamination stacks are located the PM segments, as described in [10].Each toot his wound with a coil of N turns (N = 100 in the setup of Fig. 2) and these 8 stator coils are positioned along the vertical and horizontal axes, thus forming4 electromagnet (EM) poles. The four EM coils for each of the two axis are connected in series, thus 4N coils per axis. Hence, the net air-gap flux is a combination of the bias and control fluxes. PMs provide the bias flux ϕ_{pm} in the air-gap while EM coils generate flux ϕ_c for stabilization and control. Two current amplifiers per radial HMB are required. The bias flux ϕ_{pm} generated by the PMs circulates in a loop parallel to the shaft axis while the control flux ϕ_c generated by the EMs flows radially in a loop normal to the shaft axis. Fig. 3 illustrates these two main flux paths. Neglecting the reluctance of the magnetic cores and leakage through surrounding air, a good approximate model for the electromagnetic flux can be derived using equivalent magnetic circuit. For the rotor displaced from the concentric position by a small amount y_{bA} it has been shown in [15] that the total flux in air gaps #1 and #3 can be formulated as,

$$\begin{aligned}\phi_1 &= \phi_{pm,1} + \phi_{c,1} \\ &= \frac{A_g A_m h_m B_r}{2(G - y_{bA})\mu_{rec} A_m + h_m A_g} + \mu_0 A_g \frac{2G + y_{bA}}{2G^2 - y_{bA}^2} N i_1\end{aligned} \tag{1}$$

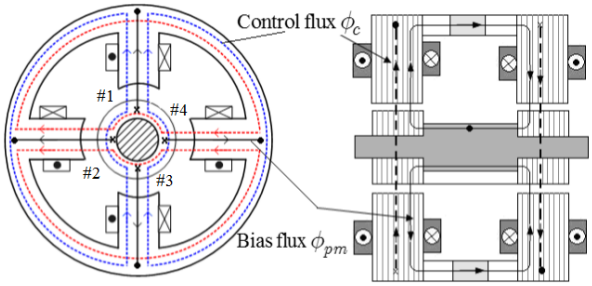

Fig. 3. The main flux paths of homopolar PM-biased magnetic bearing

$$\phi_3 = \phi_{pm,3} - \phi_{c,3} = \frac{A_g A_m h_m B_r}{2(G + y_{bA})\mu_{rec} A_m + h_m A_g} - \mu_0 A_g \frac{2G - y_{bA}}{2G^2 - {y_{bA}}^2} N i_1 \quad (2)$$

where B_r is the PM remnant flux density, h_{pm} is the axial length of PM segments, A_m is the cross section of the PM located between the two stators, A_g is the air gap area below one tooth, μ_0 is the free-space permeability, μ_{rec} is the PM relative recoil permeability and G is the air gap thickness under one tooth at equilibrium, i_1 is the current flowing in EM coils 1 and 3, and N is the number of coil turns around a pole. The vertical magnetic force F_{my} exerted on the stator by the HMB was derived in [15] and is formulated as:

$$F_{my} = F_1 - F_3 = \left(\frac{\phi_1^2}{\mu_0 A_g} - \frac{\phi_3^2}{\mu_0 A_g} \right) \quad (3)$$

The electromagnetic force in (3) is a nonlinear function of the fluxes. Taylor expansion can be used for linearization around the operating point. The linearized bearing force f_b acting along the y- axis direction can be written as:

$$F_{my} \cong F_{my}(I_{y0}, 0) + \left.\frac{\partial F_{my}}{\partial y_{bA}}\right|_{\substack{i_1 = I_{y0} \\ y_{bA} = 0}} y_{bA} + \left.\frac{\partial F_{my}}{\partial i_1}\right|_{\substack{i_1 = I_{y0} \\ y_{bA} = 0}} i_y \quad (4)$$

where I_{yo} is a constant current needed to fight gravitation forces acting on the bearing shaft. Thus, the first term in (4) will be cancelled by the static load which is equal to half of the weight in the vertical direction and zero in the horizontal direction. For the vertical direction, the force acting at the operating point can be written as

$$F_{my} \cong F_{my}(I_{y0}, 0) + \Delta F_{my}$$

where the incremental force ΔF_{my} can formulated as

$$\Delta F_{my} = -k_{sy} y_{bA} + k_{iy} i_y \quad (5)$$

where displacement stiffness k_{sy} and the force to current factor k_{iy} for the vertical direction can be respectively written[15] as:

$$k_{sy} = -\left.\frac{\partial F_{my}}{\partial y_{bA}}\right|_{\substack{i_1 = I_{y0} \\ y_{bA} = 0}} = -\left\{ \frac{2 A_g {I_{y0}}^2 N^2 \mu_0}{G^3} + \frac{8 \mu_{rec} A_g A_{pm} B_{pm}^2}{\mu_0 \left(2 G \mu_{rec} A_{pm} + h_{pm} A_g \right)} \right\} \quad (6)$$

$$k_{iy} = \left.\frac{\partial F_{my}}{\partial i_1}\right|_{\substack{i_1 = I_{y0} \\ y_{bA} = 0}} = \frac{4 N A_g B_{pm}}{G} \quad (7)$$

where B_{pm} is the flux density due to PMs, I_{y0} is the bias current, i_y is the control current in the vertical direction. Similarly, the incremental horizontal magnetic force of the HMB can formulated as

$$\Delta F_{mx} = -k_{sx} x_{bA} + k_{ix} i_x \quad (8)$$

It should be noted that the derivation of the above equations is based on assuming that the deviation of the rotor from the concentric position is less than 0.1 the width of the air-gap G and hence neglecting the electromagnetic cross coupling between the horizontal and vertical directions [15]. In other words, the cross coupling outside this region becomes significant and hence the behavior may not be well predicted by the linearized formula.

B. The Rotor-Bearing System Model

It is assumed that the rotor is symmetric and rigid, and the axial motion is decoupled from the radial ones. Therefore the radial dynamics can be represented by 4 degrees of freedom (DOF) while the axial dynamics is 1-DOF which is not being of particular interest here. The most straightforward approach to describe the rigid body dynamics is to use the shaft radial displacements x_s, y_s of its center of gravity and its inclinations angles α, β with respect to the inertial fixed reference [13]. Fig. 4 shows the basic structure of the rotor-bearing system. Before the equations of motion are given, the following coordinate systems is defined as follows

$\mathbf{q} = [\beta, x_s, -\alpha, y_s]^T$: Vector of generalized rotor coordinates

$\mathbf{q}_b = [x_{bA}, x_{bB}, y_{bA}, y_{bB}]^T$: Bearings A and B coordinate

$\mathbf{q}_{se} = [x_{seA}, y_{seA}]^T$: Sensors coordinate at bearing A

Transformations for bearing and sensor coordinates can be done according to the following relations

$$\mathbf{q_b} = \mathbf{B^T}.\mathbf{q} \quad \text{and} \quad \mathbf{q}_{se} = \mathbf{C^T}.\mathbf{q}$$

The equation of motion for a rotor suspended with a HMB and a ball bearing can be written as

$$\mathbf{M}\ddot{\mathbf{q}} + \omega \mathbf{G}\dot{\mathbf{q}} = \mathbf{B}(\mathbf{F_m} + \mathbf{F_b}) + \mathbf{F_{un}} \quad (9)$$

$$\mathbf{y} = \mathbf{q}_{se} \quad (10)$$

where the gravitation term was left out for simplification and where

$$\mathbf{M} = \begin{bmatrix} J_y & 0 & 0 & 0 \\ 0 & m & 0 & 0 \\ 0 & 0 & J_x & 0 \\ 0 & 0 & 0 & m \end{bmatrix}, \ \mathbf{G} = \begin{bmatrix} 0 & 0 & J_z & 0 \\ 0 & 0 & 0 & 0 \\ -J_z & 0 & 0 & 0 \\ 0 & 0 & 0 & 0 \end{bmatrix}$$

$$\mathbf{B} = \begin{bmatrix} -a & b & 0 & 0 \\ 1 & 1 & 0 & 0 \\ 0 & 0 & -a & b \\ 0 & 0 & 1 & 1 \end{bmatrix}, \ \mathbf{C} = \begin{bmatrix} -c & 0 \\ 1 & 0 \\ 0 & -c \\ 0 & 1 \end{bmatrix}$$

where m is the rotor mass, J_x, J_y and J_z are the moments of inertia of the rotor around x, y, z axis respectively, ω is the rotation speed. Lengths a and b are the distance between the bearings and COG (O) while c is the distance between the sensor coordinates and COG. $\boldsymbol{M}$ and $\boldsymbol{G}$ are the mass and gyroscopic matrices respectively. The compensation electromagnetic force vector $\boldsymbol{F_m}$ can be derived from (5)-(8) as:

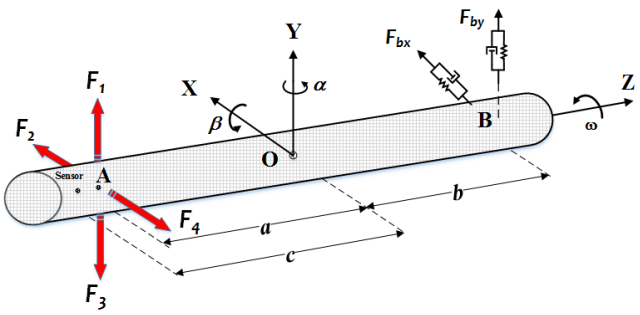

Fig. 4 Basic structure of the rotor-bearing system

$$\begin{aligned}\mathbf{F}_m &= \begin{bmatrix}\Delta F_{mx} & 0 & \Delta F_{my} & 0\end{bmatrix}^T \\ &= -\mathbf{K}_s\mathbf{q}_b + \mathbf{K}_i\mathbf{i} \\ &= -\mathbf{K}_s\mathbf{B}^T\mathbf{q} + \mathbf{K}_i\mathbf{i}\end{aligned} \tag{11}$$

where

$\mathbf{K_s} = diag[k_{sx},\ 0,\ k_{sy},\ 0]$, $\mathbf{K_i} = diag[k_{ix},\ 0,\ k_{iy},\ 0]$

$\mathbf{i} = [i_x,\ 0,\ i_y,\ 0]$

The mechanical ball bearing force vector can be approached from [16] as

$$\begin{aligned}\mathbf{F}_b &= \begin{bmatrix}0 & \Delta F_{bx} & 0 & \Delta F_{by}\end{bmatrix} \\ &= -\mathbf{K}_{bb}\mathbf{B}^T\mathbf{q} - \mathbf{C}_{bb}\mathbf{B}^T\dot{\mathbf{q}}\end{aligned} \tag{12}$$

where

$$\mathbf{K}_{bb} = diag\begin{bmatrix}0 & k_{xx} & 0 & k_{yy}\end{bmatrix},\ \mathbf{C}_{bb} = diag\begin{bmatrix}0 & c_{xx} & 0 & c_{yy}\end{bmatrix}$$

k_{xx}, and k_{yy} represent the stiffness in the horizontal and vertical directions respectively while c_{xx}, and c_{yy} represent the damping effect in the horizontal and vertical directions respectively.

The static unbalance forces acting on the system at the COG in x and y directions respectively can be modeled as in [16]

$$\mathbf{F}_{un} = \begin{bmatrix}0 & m_e\varepsilon\omega^2\cos(\omega t) & 0 & m_e\varepsilon\omega^2\sin(\omega t)\end{bmatrix} \tag{13}$$

where m_e represents the unbalance mass while ε represents the offset of m_e from the COG. It is assumed that $m_e\varepsilon = 0.01\ kg.m$. These unbalance forces cause vibrations in the rotating shaft and the amplitude of these vibrations is proportional to the square of rotational speed ω.

Substituting for (11) and (12) in (9) and after manipulations gives

$$\begin{aligned}&\mathbf{M}\ddot{\mathbf{q}} + \left(\omega\mathbf{G} + \mathbf{B}\mathbf{C}_{bb}\mathbf{B}^T\right)\dot{\mathbf{q}} + \left(\mathbf{B}\mathbf{K}_s\mathbf{B}^T + \mathbf{B}\mathbf{K}_{bb}\mathbf{B}^T\right)\mathbf{q} \\ &= \mathbf{B}\mathbf{K}_i\mathbf{i} + \mathbf{F}_{un}\end{aligned} \tag{14}$$

III. Sliding Mode Control Design

In this section we will consider Sliding Mode Control (SMC) for controlling the HMB in one direction. The decentralized control structure approach is followed in this paper, so two decentralized SMC loops are required to control each direction. But first we need to decouple the rotor-HMB dynamics into two 1-DOF systems.

A. 1-DOF Hybrid Magnetic Suspension System

The following assumption are set to simplify the Rotor-bearing modeling (14):

- The rotor-bearing system is rigid and symmetric.
- To achieve 1-DOF, the system is at standstill.
- Sensors and bearings are collocated.
- Any coupling between the two bearings in x-z plane and in y-z plane are neglected.

and then the Rotor-HMB interaction can be reduced into two simple 1-DOF magnetic suspension system

$$\frac{m}{2}\ddot{x}_s + k_s\,x_s = k_i\,i_x \tag{15}$$

$$\frac{m}{2}\ddot{y}_s + k_s\,y_s = k_i\,i_y \tag{16}$$

and from (10), $x_{seA} = x_s - c\beta$ and $y_{seA} = y_s + c\alpha$

B. Sliding Mode Control

SMC is a particular type of variable structure control systems (VSCS) which is characterized by a suite of feedback control laws and a decision rule (also known as switching function)[17]. The switching function is tailored so that the sliding motion satisfies the design requirements while the job of control law is to ensure that the state trajectories are driven towards and remain thereafter on the sliding manifold to guarantee a sliding motion. SMC has been attracting the attention of researchers since 1960's due to its order reduction property and its low sensitivity to disturbances and plant parameter variations [18]. In other words, SMC is an efficient tool to control non-linear dynamic systems under uncertainty conditions. As the HMB is non-linear and unstable, SMC is of particular interest.

If the displacement and velocity are chosen as the states of the system ($z_1 = x_{seA}$ and $z_2 = \dot{x}_{seA}$) and the current is control input ($u = i_x$), (15)-(16) can be generalized into a state space representation as follows:

$$\begin{cases}\begin{bmatrix}\dot{z}_1 \\ \dot{z}_2\end{bmatrix} = \begin{bmatrix}0 & 1 \\ \dfrac{-2k_s}{m} & 0\end{bmatrix}\begin{bmatrix}z_1 \\ z_2\end{bmatrix} + \begin{bmatrix}0 \\ \dfrac{2k_i}{m}\end{bmatrix}u + f(t,z,u) \\ y_m = z_1\end{cases} \tag{17}$$

or in compact form as

$$\dot{\mathbf{z}} = \mathbf{A}\,\mathbf{z} + \mathbf{D}\,\mathbf{u} + f(t,z,u) \tag{18}$$

where the function f represents the uncertainty in the system which is assumed to be unknown but bounded, i.e., $\left|f(t,z,u)\right| \le P$.

In (15)-(18), the system model is linearized around an equilibrium point (here the geometrical center of the safety bearing). It is the aim of the designed controller to be able to follow a reference y_r. The output tracking error e should be minimized. The latter is defined by (19) as:

$$e = y_r - y_m \tag{19}$$

Substituting for (19) in (17) and after manipulation, we get

$$\dot{\Psi} = \mathbf{A}\,\Psi + \mathbf{D}\mathbf{u} + \gamma\left(t, z, y_c, u\right) \tag{20}$$

where $\Psi = \begin{bmatrix} e & \dot{e} \end{bmatrix}^T$ and $\gamma\left(t, z, y_r, u\right) = \dfrac{2k_s}{m} y_r + f\left(t, z, u\right)$

The objective is to design a SMC u to derive the tracking error to zero. The design of a SMC comprises two steps. First, the design of the sliding variable so that the dynamics of reduced order system satisfies the required performance. Second, selection of a discontinuous control law that makes the sliding variable is attractive to the tracking error trajectories in the presence of bounded uncertainties. A good candidate for the switching variable σ is

$$\sigma = \zeta e + \dot{e} = \mathbf{S}\,\Psi \tag{21}$$

where $\mathbf{S} = \begin{bmatrix} \zeta & 1 \end{bmatrix}$ and ζ is a design variable. A common SMC structure is composed of a linear component u_{eq} and a discontinuous component u_n as follows

$$\mathbf{u} = \mathbf{u_{eq}} + \mathbf{u_n} \tag{22}$$

The linear component u_{eq} which is the equivalent control action necessary to maintain an ideal sliding motion on σ. To calculate u_{eq}, it is assumed that the uncertain function *f(t,z,u)*is initially equal to zero. The error states reach the sliding variable σ after a finite time t_r which means that σ= 0and $\dot{\sigma} = 0$ so

$$-\mathbf{S}\dot{\mathbf{e}} = -\mathbf{S}\mathbf{A}\mathbf{e} + \mathbf{S}\mathbf{D}u = 0$$

and thus

$$\mathbf{u_{eq}} = \mathbf{(SD)^{-1}SA\,e} \tag{23}$$

Choose the nonlinear component as

$$\mathbf{u_n} = (\mathbf{SD})^{-1}\rho\,\mathrm{sgn}(\sigma) \quad , \rho > 0 \tag{24}$$

where ρ is a design variable. Then it follows that

$$\begin{aligned} \sigma\dot{\sigma} &= \sigma\mathbf{S}(\mathbf{Ae} - \mathbf{Du}) \\ &= \sigma\mathbf{SAe} - \sigma\mathbf{SD}\left[(\mathbf{SD})^{-1}\mathbf{SAe} + (\mathbf{SD})^{-1}\rho\,\mathrm{sgn}(\sigma)\right] \\ &= -\sigma\mathbf{SAe} + \sigma\mathbf{SAe} - \sigma\rho\,\mathrm{sgn}(\sigma) \\ &= -\rho\sigma\,\mathrm{sgn}(\sigma) \\ &\le -\rho\left|\sigma\right| \end{aligned} \tag{25}$$

and hence the reachability condition is satisfied [17], [19]. Despite the discontinuous function $\mathrm{sgn}(\sigma)$ achieves an ideal sliding motion, it causes a chattering problem which is undesirable in practice. A common solution to this problem is to let the states remain in an arbitrary boundary layer in the neighborhood of the surface σ rather than forcing the error states to stay on it. One possible option is to select an approximate continuous function as

$$\mathbf{u_n} = (\mathbf{SD})^{-1}\rho\frac{\sigma}{\left|\sigma\right| + \delta} \tag{26}$$

Table I MODEL DATA FOR ROTOR-BEARING SYSTEM

Rotor mass (m)	61.9 kg
Rotor transverse moment of inertia (J_x = J_y)	4.79 kg m^2
Rotor polar moment of inertia (J_z)	0.086 kg m^2
Force to current factor (k_{ix} = k_{iy})	609 N/A
HMB stiffness for horizontal motion (k_{sx})	-28.05 N/mm
HMB stiffness for vertical motion (k_{sy})	-47.8 N/mm
Nominal HMB air-gap length (G)	1 mm
Nominal safety bearing clearance length	0.5 mm
Bias current for vertical direction (I_{y0})	0.5 A
Bias current for horizontal coils (I_{x0})	0 A

where δ is the boundary layer. A tradeoff is necessary in tuning δ to reduce the chattering while maintaining an ideal performance.

IV. Simulation and Performance Evaluation

Simulation is done in MATLAB Simulink, to determine how Sliding Mode Control can be compared with standard linear PID controller for regulating the position in a HMB dedicated to the Wayside Energy Storage System with low self-discharge. The rotor-bearing system is modeled according to (14). Table I indicates the model data used in this work. It is assumed that the system operates at a rotating speed $\omega = 3600$ RPM. The sampling time is 0.1ms.

The objective is to regulate the rotor at the operating speed despite these unbalance forces. Displacements should not exceed 30% of the safety bearing clearance, i.e. 0.15 mm. The variations of the control currents are constrained between ± 2 A. Table II shows the design parameters for the PID and SMC controllers used in simulation study.Fig. 5 shows a comparison between the SMC and PID controller to a step response of 0.1 mm applied to the horizontal axis of Bearing A at $\omega = 0$ RPM. For the PID controller, there is a 30% overshoot and the system settles after 0.02 second. For The SMC, there is no overshoot since the closed loop system behaves as a first order system due to the dynamic collapse and the settling time is 30 ms. Fig. 6 shows the rotor orbits at bearing A for a rotation speed of 3600 RPM and demonstrates the success of the SMC to achieve the required objective while the PID controller fails. Fig. 7 shows that the control currents for both PID and SMC

Table II DESIGN PARAMETERS FOR PID AND SMC

		Horizontal Direction	Vertical Direction
PID Control	K_p	3500	4000
	K_i	15000	40000
	K_d	10	20
SMC Control	ζ	100	100
	ρ	20	20
	δ	0.01	0.01

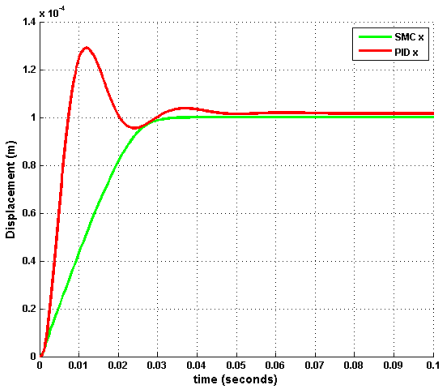

Fig. 5 Step Response

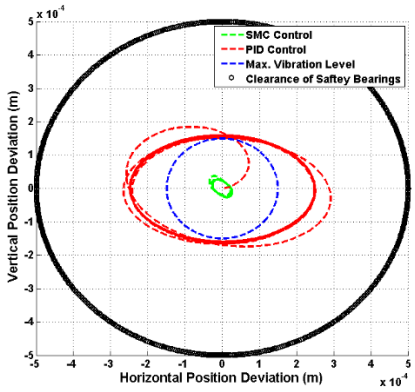

Fig.6 Rotor Orbit at 3600 RPM rotation speed

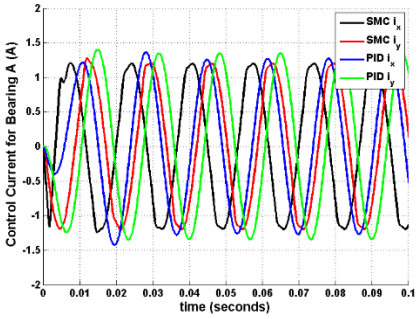

Fig.7 Control Currents at 3600 RPM rotation speed

controlled system. We can conclude that the output tracking and vibration attenuation performances of the SMC are superior over the conventional PID controller.

V. Conclusion

A Sliding Mode Control for regulating a rotor supported on an energy-efficient Hybrid Magnetic Bearing is addressed in this paper. This magnetic bearing is a good potential for employing long-term FESS for Wayside Energy Storage. Simulation results show the efficiency of the SMC for achieving smooth output tracking with a settling time of 0.03s. The controller also succeeds in attenuating the vibration magnitude to 30 µm at 3600 rpm rotation speed. The performacne The control approach presented in the paper indicates good potential for using HMB in long-term FESS applications. The next step is to implement experimentally the SMC on our practical setup and evaluate the closed loop performance in future publication.

References

[1] C. Lamontagne, "Advanced Wayside Energy Storage Systems for Rail Transit," Transit IDEA Prog., Burlington, MA, Project 66, Final Rep., 2013.

[2] M. L. Pastor, L. G.-T. Rodriguez, and C. V. Velez, "FlyWheels Store to Save," *IEEE Electrif. Mag.*, vol. 1, pp. 13–20, 2014.

[3] V. Gelman, "Comparison Between Wayside Storage and Reversible Thyristor Controlled Rectifiers (RTCR) for Heavy Rail Applications," in *2013 Joint Rail Conference*, 2013, pp. V001T07A001–V001T07A001.

[4] S. Vazquez, S. M. Lukic, E. Galvan, L. G. Franquelo, and J. M. Carrasco, "Energy Storage Systems for Transport and Grid Applications," *IEEE Trans. Ind. Electron.*, vol. 57, no. 12, pp. 3881–3895, 2010.

[5] I. Hadjipaschalis, A. Poullikkas, and V. Efthimiou, "Overview of current and future energy storage technologies for electric power applications," *Renew. Sustain. Energy Rev.*, vol. 13, no. 6, pp. 1513–1522, 2009.

[6] H. Ibrahim, A. Ilinca, and J. Perron, "Energy storage systems—characteristics and comparisons," *Renew. Sustain. Energy Rev.*, vol. 12, no. 5, pp. 1221–1250, 2008.

[7] A. Kusko and J. DeDad, "Stored energy-Short-term and long-term energy storage methods," *Ind. Appl. Mag. IEEE*, vol. 13, no. 4, pp. 66–72, 2007.

[8] G. Joos, M. De Freige, and M. Dubois, "Design and simulation of a fast charging station for PHEV/EV batteries," in *EPEC 2010 - IEEE Electrical Power and Energy Conference: "Sustainable Energy for an Intelligent Grid,"* 2010.

[9] "Long Term Storage flywheel," *TU Wien - Institut für Mechanik und Mechatronik*. [Online]. Available: http://www.mec.tuwien.ac.at/messtechnik_und_aktorik/messtechnik_und_aktorik/forschung/projekte/flywheel/. [Accessed: 23-Feb-2015].

[10] L. Bakay, M. Dubois, P. Viarouge, and J. Ruel, "Losses in hybrid and active magnetic bearings applied to Long Term Flywheel Energy Storage," *Power Electronics, Machines and Drives (PEMD 2010), 5th IET International Conference on*. pp. 1–6, 2010.

[11] C. Sortore, P. Allaire, and E. Maslen, "Permanent magnet biased magnetic bearings, design, construction and testing," *Second Int. Symp. Magn. Bear.*, 1990.

[12] Y. Fan, A. Lee, and F. Hsiao, "Design of a permanent/electromagnetic magnetic bearing-controlled rotor system," *J. Franklin Inst.*, vol. 334, no. 3, 1997.

[13] H. Bleuler, M. Cole, P. Keogh, R. Larsonneur, E. Maslen, Y. Okada, G. Schweitzer, A. Traxler, and E. H. Maslen, *Magnetic Bearings: Theory, Design, and Application to Rotating Machinery*. Berlin, Heidelberg: Springer Berlin Heidelberg, 2009.

[14] S. Y. Yoon, Z. Lin, and P. E. Allaire, *Control of Surge in Centrifugal Compressors by Active Magnetic Bearings*. London: Springer London, 2013.

[15] A.-C. Lee, F.-Z. Hsiao, and D. Ko, "Analysis and Testing of Magnetic Bearing with Permanent Magnets for Bias," *JSME Int. journal. Ser. C, Dyn. Control. Robot. Des. Manuf.*, vol. 37, no. 4, pp. 774–782, 1994.

[16] G. Genta, *Dynamics of Rotating Systems*. Springer, 2005.

[17] C. Edwards and S. Spurgeon, *Sliding Mode Control: Theory And Applications*. Taylor & Francis, 1998.

[18] V. Utkin, J. Guldner, and J. Shi, *Sliding Mode Control in Electro-Mechanical Systems*, 2nd ed. CRC press, 2009.

[19] Y. Shtessel, C. Edwards, L. Fridman, and A. Levant, *Sliding Mode Control and Observation*. New York, NY: Springer New York, 2014.